IJST, Transactions of Mechanical Engineering, Vol. 39, No. M1+, pp 185-196
Printed in The Islamic Republic of Iran, 2015


# AN INVESTIGATION ON THE ENERGY ABSORPTION OF ALUMINUM FOAM CORE SANDWICH PANEL VIA QUASI-STATIC PERFORATION TEST*

M. GOLESTANIPOUR, A. BABAKHANI AND S. M. ZEBARJAD**

Dept. of Materials and Metallurgical Engineering, Faculty of Engineering, Ferdowsi University of Mashhad, P.O. Box 91775-1111, Mashhad, I. R. of Iran
Email: zebarjad@um.ac.ir

**Abstract–** Aluminum foams are a novel branch of advanced materials with superior properties. Sandwich structures with aluminum foam core are good energy absorbers. In this paper, mechanical properties and energy absorption of aluminum foam sandwich panels subjected to quasi-static perforation tests with conical-nosed indenter were investigated experimentally. For this purpose sandwich panels consisting of two aluminum face-sheets and a closed cell aluminum foam core were fabricated. Quasi-static perforation tests on fully fixed sandwich panels were carried out by a universal testing machine at a cross head speed of 0.02 mm/s. Force-displacement curves were recorded and peak piercing force and absorbed energy of sandwich panels were calculated accordingly. Effects of foam core density (0.5, 0.6 and 0.7 g/cm$^3$) and thickness of face-sheets (0.6, 1 and 2 mm) and foam core (10, 20 and 30 mm) on the mechanical properties and energy absorption of samples were discussed. The results showed that increasing foam core and face-sheet thickness and foam core density led to more total absorbed energy being achieved and higher piercing force.

**Keywords–** Sandwich panel, aluminum foam, perforation, energy absorption

## 1. INTRODUCTION

Metallic foams are a novel branch of engineering materials with low densities and novel mechanical, physical, thermal, acoustic and electrical properties. These advanced, relatively cheap materials offer applications for lightweight structures, energy absorption, and thermal management. Aluminum foam sandwich panels typically consist of two solid face-sheets with high strength and a low density aluminum foam core. The foam core has the ability of undergoing large deformation at a relatively constant stress, while the face-sheets provide stretching and bending capacity. Thus sandwich panels can dissipate and absorb a relatively large amount of kinetic energy before collapsing into a more stable configuration. Sandwich panels with aluminum foam core are low weight and good energy absorbers offering a broad range of applications in aerospace, marine and automotive industries. Owing to the relatively low strength of the foam core and thin face sheets, aluminum foam sandwich panels are prone to causing local indentation under concentrated loads such as handling, interaction with attached structures or impact. Researches have indicated that indentation behavior of sandwich panels with foam cores is mainly affected by some factors such as the foam core material, face sheet thickness and indenter size [1-7].

Impact response of ALPORAS® foam sandwich panels, fibre-metal laminate (FML) and fibre-reinforced thermoplastic face-sheets was investigated by Cantwell and Kiratisaevee [6]. Impact perforation tests were also carried out using a 3 m/s velocity drop hammer. The indentation force of sandwich panels was found to be rate sensitive.

---

*Received by the editors August 23, 2014; Accepted November 15, 2014.
**Corresponding author

Quasi-static perforation tests using both flat and spherical punches were carried out by Mohan et al. [7]. They used ALPORAS® aluminum foam sandwich panels with aluminum, stainless steel, CFRP matrix composite face-sheets. Core indentation, core crushing, face-sheet punching and face-sheet bending were four failure modes in these tests.

Experimental and finite element simulations on CYMAT® sandwich panels subjected to both quasi-static and impact loadings using a hemi-spherical indenter were conducted by Lu et al. [8]. Global bending, localized indentation, localized indentation with global bending, and localized indentation with bending along clamping edge were summarized as four deformation modes.

Ruan et al. [9] discussed the effects of core and face-sheet thickness, surface condition of face-sheets, boundary conditions, and adhesive on the mechanical properties and absorbed energy of sandwich panels with ALPORAS® foam core. They showed that thicker face-sheet, thicker core, higher degree of constraint and abraded face-sheets resulted in higher absorbed energy.

The quasi-static perforation tests were carried out using flat ended, hemispherical-nosed and conical-nosed punches by Hou et al. [10]. They found that thicker face-sheets and the cores with higher thickness and density resulted in higher energy absorption being produced. Thicker face-sheets also resulted in a larger delamination area between the core and back face. The tests were carried out on sandwich panels with CYMAT® aluminum foam core and 5005H34 aluminum face-sheets with different thicknesses and core relative densities.

Local indentation properties of sandwich panels were analyzed according to the principle of minimum potential energy by Xie et al. [11]. Their analytical results were verified by those from ABAQUS code simulation, and they were in good agreement. Distribution of tensile strain of the upper face sheet and the energy dissipation of foam core to that of the upper face sheet was also analyzed.

Altenaiji et al. [12] presented a study on aluminum matrix foams as a possible core material for a protection system on military vehicles. Characterization of the foam behavior under low velocity impact loading and identification of the underlying failure mechanisms were carried out to evaluate the effective mechanical performance. They found that samples subjected to drop weight impact offered 20-30% higher plateau stresses than those of the samples subjected to quasi-static compression loading.

Relative performance of metal and polymeric foam cored sandwich plates was studied under low velocity impact loading by Rajaneesh et al. [13]. They studied peak force, energy absorption values and failure mode patterns by analytical estimation techniques, experimental measurements and numerical predictions.

In this research, quasi-static perforation experiments were conducted on sandwich panels with Al/SiCp composite foam core and 1100 aluminum alloy face-sheets using a ZWICK Z250 universal testing machine. Specimens were placed fully fixed in a special fixture. Force-displacement curves were recorded and maximum piercing force and total absorbed energy of sandwich panels were accordingly calculated. Effects of face-sheet thickness and foam core thickness and density were discussed.

## 2. EXPERIMENTAL PROCEDURE

### *a) Materials*

The produced sandwich panels consisted of top face-sheet, bottom face-sheet and core material. The core material of sandwich panels was closed-cell Al A356/10 wt.% SiCp composite foam provided by ACECR, Mashhad, Iran [14, 15]. Foam cores with the density of 0.5, 0.6 and 0.7 g/cm$^3$ were cut into 120 mm×120 mm plates with 10, 20 and 30 mm thicknesses. The density of a homogeneous foam structure equals its mass divided by its volume. The foam mass was measured with a scale and the volume was calculated directly from the geometry of the foam block. The top and bottom face-sheets were made of 1100 aluminum alloy with 0.6, 1.0 and 2.0 mm thicknesses. Core-absent specimens (two identical faces with 30 mm air core) and foams without face-sheet were prepared as witness samples to evaluate the effect of face-sheets and foam core on energy absorption separately. Face-sheets were bonded to the core material using Akfix 610 polyurethane base adhesive. The adhesive film was cured in ambient temperature for 24 hours. Maximum bonding strength was achieved after this curing time. Figure 1 schematically illustrates the preparation procedure of the sandwich panels. A produced panel with its different parts, an image from a cross section of a specimen, and a scanning electron micrograph of foam core fracture surface are respectively shown in Fig. 2a, 2b and 2c. It can be found that the distribution of cells is relatively uniform and foam core has a homogenous microstructure. The nomenclature and properties of all samples are given in Table 1.

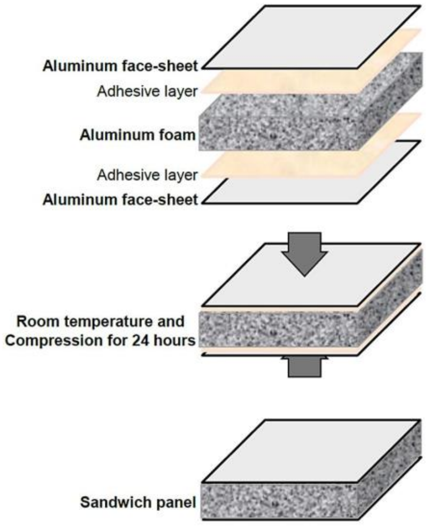


Fig. 1. Preparation procedure of the sandwich panels

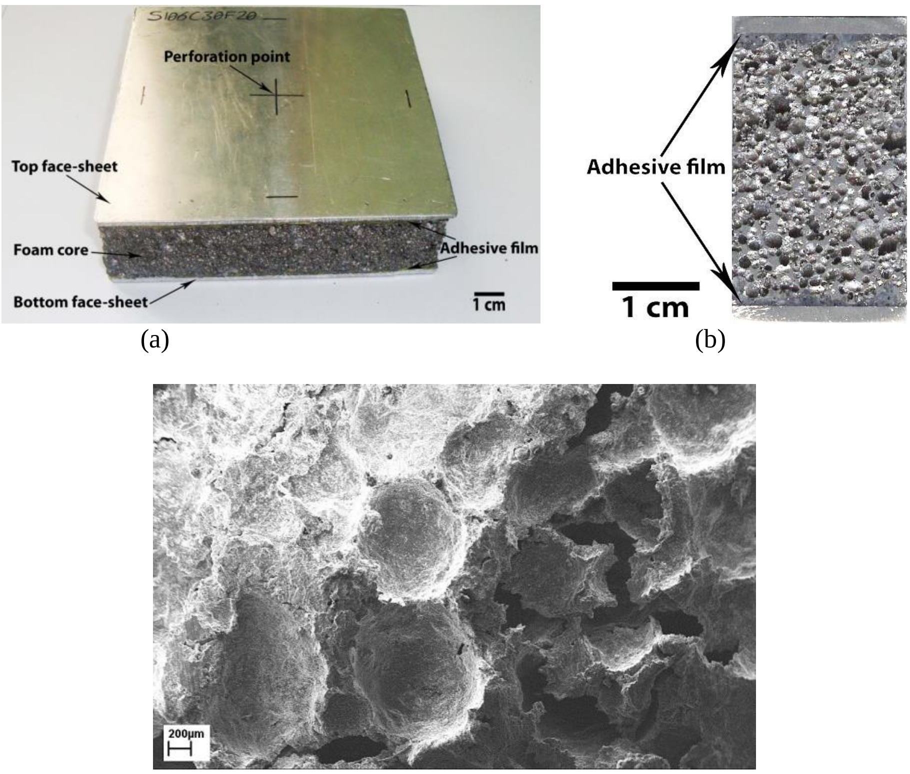


(a) (b)

(c)

Fig. 2. a) A produced sandwich panel with its different parts, b) an image from cross section of a specimen, and c) a scanning electron micrograph of foam core fracture surface

Table 1. Nomenclature and properties of produced specimens

| Nomenclature | Foam core density ($g/cm^3$) | Foam core thickness (mm) | Face-sheet thickness (mm) | Sample weight (kg) | Peak piercing force (N) | Total absorbed energy (J) | Specific absorbed energy (J/kg) |
|---|---|---|---|---|---|---|---|
| 105C10F00 | 0.5 | 10 | 0 | 0.061 | 572.56 | 4.224 | 69.82 |
| 105C10F06 | 0.5 | 10 | 0.6 | 0.143 | 2287.37 | 30.73 | 214.90 |
| 105C10F10 | 0.5 | 10 | 1 | 0.167 | 3344.08 | 60.53 | 362.46 |
| 105C10F20 | 0.5 | 10 | 2 | 0.250 | 5019.7 | 116.85 | 467.40 |
| 105C20F00 | 0.5 | 20 | 0 | 0.159 | 1005.09 | 10.227 | 64.52 |
| 105C20F06 | 0.5 | 20 | 0.6 | 0.221 | 2837.62 | 50.57 | 228.82 |
| 105C20F10 | 0.5 | 20 | 1 | 0.256 | 3518.52 | 80.71 | 315.89 |
| 105C20F20 | 0.5 | 20 | 2 | 0.338 | 5326.44 | 123.98 | 366.80 |
| 105C30F00 | 0.5 | 30 | 0 | 0.172 | 1023.79 | 16.73 | 97.55 |
| 105C30F06 | 0.5 | 30 | 0.6 | 0.270 | 2826.22 | 83.64 | 309.78 |
| 105C30F10 | 0.5 | 30 | 1 | 0.334 | 3730.25 | 105.62 | 316.23 |
| 105C30F20 | 0.5 | 30 | 2 | 0.398 | 5512.15 | 147.68 | 371.06 |
| 106C10F00 | 0.6 | 10 | 0 | 0.083 | 691.88 | 6.268 | 75.52 |
| 106C10F06 | 0.6 | 10 | 0.6 | 0.154 | 2720.29 | 41.65 | 270.45 |
| 106C10F10 | 0.6 | 10 | 1 | 0.186 | 4190.42 | 74.18 | 398.82 |
| 106C10F20 | 0.6 | 10 | 2 | 0.261 | 6752.43 | 136.11 | 521.49 |
| 106C20F00 | 0.6 | 20 | 0 | 0.171 | 1677.95 | 22.936 | 134.52 |
| 106C20F06 | 0.6 | 20 | 0.6 | 0.232 | 2914.66 | 60.07 | 258.92 |
| 106C20F10 | 0.6 | 20 | 1 | 0.277 | 4124.02 | 110.12 | 398.26 |
| 106C20F20 | 0.6 | 20 | 2 | 0.355 | 6872.7 | 144.62 | 407.95 |
| 106C30F00 | 0.6 | 30 | 0 | 0.258 | 1966.21 | 27.647 | 107.37 |
| 106C30F06 | 0.6 | 30 | 0.6 | 0.309 | 3846.62 | 96.61 | 312.65 |
| 106C30F10 | 0.6 | 30 | 1 | 0.368 | 4552.86 | 124.13 | 337.31 |
| 106C30F20 | 0.6 | 30 | 2 | 0.410 | 6762.96 | 195.43 | 476.66 |
| 107C10F00 | 0.7 | 10 | 0 | 0.107 | 1280.77 | 17.56 | 164.11 |
| 107C10F06 | 0.7 | 10 | 0.6 | 0.165 | 2878.88 | 33.09 | 200.55 |
| 107C10F10 | 0.7 | 10 | 1 | 0.211 | 4495.6 | 71.51 | 338.91 |
| 107C10F20 | 0.7 | 10 | 2 | 0.277 | 6668.71 | 146.81 | 530.00 |
| 107C20F00 | 0.7 | 20 | 0 | 0.220 | 1452.18 | 17.47 | 79.59 |
| 107C20F06 | 0.7 | 20 | 0.6 | 0.268 | 4484.14 | 85.25 | 318.10 |
| 107C20F10 | 0.7 | 20 | 1 | 0.313 | 5976.08 | 125.06 | 399.55 |
| 107C20F20 | 0.7 | 20 | 2 | 0.374 | 7316.14 | 150.37 | 402.06 |
| 107C30F00 | 0.7 | 30 | 0 | 0.297 | 1737.87 | 29.697 | 100.16 |
| 107C30F06 | 0.7 | 30 | 0.6 | 0.353 | 4351.36 | 111.41 | 315.61 |
| 107C30F10 | 0.7 | 30 | 1 | 0.400 | 6059.02 | 146.76 | 366.90 |
| 107C30F20 | 0.7 | 30 | 2 | 0.476 | 7548.95 | 229.22 | 481.55 |
| 000C00F06 | 0 | 0 | 0.6 | 0.127 | 551.92 | 14.997 | 118.55 |
| 000C00F10 | 0 | 0 | 1 | 0.155 | 1280.23 | 40.099 | 259.54 |
| 000C00F20 | 0 | 0 | 2 | 0.253 | 3479.56 | 104.08 | 411.38 |

### *b) Quasi-static perforation tests*

A ZWICK Z250 universal testing system was used to perform the quasi-static perforation tests. Specimens were fully fixed at the edges using two steel frames, which had a 100 mm diameter circular opening in the center and were placed on the bottom platen of testing machine (Fig. 3). A 10 mm diameter conical nosed indenter moved down to pierce the specimens at a velocity of 0.02 mm/s for all tests. The force-displacement data were recorded automatically by the computer connected to the machine. Each test was carried out three times to ensure reliability.

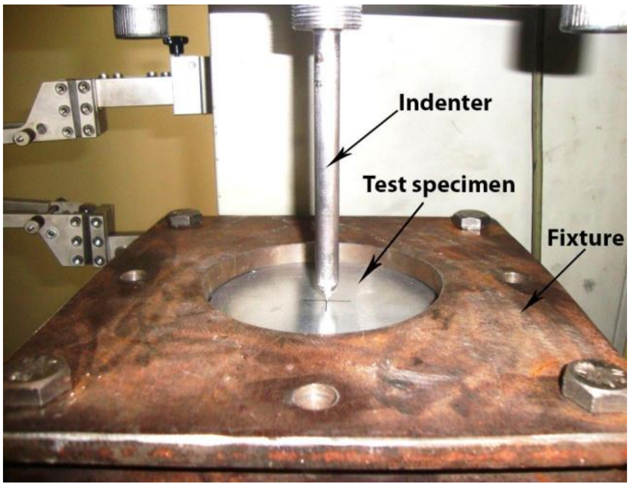


Fig. 3. Quasi-static perforation test setup

## 3. RESULTS AND DISCUSSION

The quasi-static engineering tensile stress-strain curves of the face-sheets based on ASTM E8 standard are exhibited in Fig. 4a. It is clear that the thicker face-sheets have a higher resistance against tensile force and so fracture occurs at higher level of stress. Compression stress-strain curves of the foam cores according to DIN 50134 standard are also exhibited in Fig. 4b. It is seen that the stress depends strongly on density. SiC particles in cell walls can support the stress until it becomes sufficiently large and causes damage by the failure either at or near the interface, or by the fracture of particles. The results show that with increasing density higher compressive strength is achieved. Just like other closed cell metallic foams, composite foams have characteristic compressive stress-strain curves, i.e. they involve three distinct stages: linear elastic deformation region, collapse plateau region and densification region.

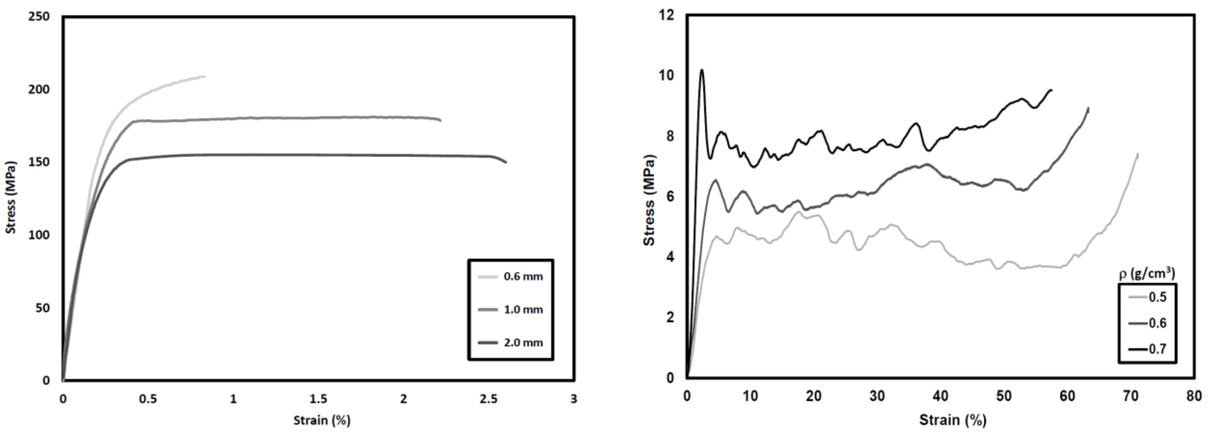


(a) (b)

Fig. 4. Quasi-static engineering stress-strain curves of a) face-sheets and b) foam cores

***a) Force-displacement curve***

Piercing force-displacement curves of sandwich structures with 0.7 g/cm$^3$ foam core density for 10, 20 and 30 mm foam core thicknesses are respectively shown in Fig. 5a, 5b and 5c. All curves demonstrated the following three stages:

1) *Front face failure:* the contact force between the indenter and specimen sharply increases from zero to the first peak, then drops quickly, implying the sudden failure of the front face;

2) *Core failure:* the piercing force reaches minimum and exhibits a plateau, indicating the core failure due to shear and a small amount of compression; and

3) *Back face failure:* the force goes up again to the relatively lower second peak, where the core becomes densified and then the back face fails. This second peak is negligible for panels with thin face-sheets. When the indenter penetrates the back face, the force drops to zero gradually, due to the friction effect.

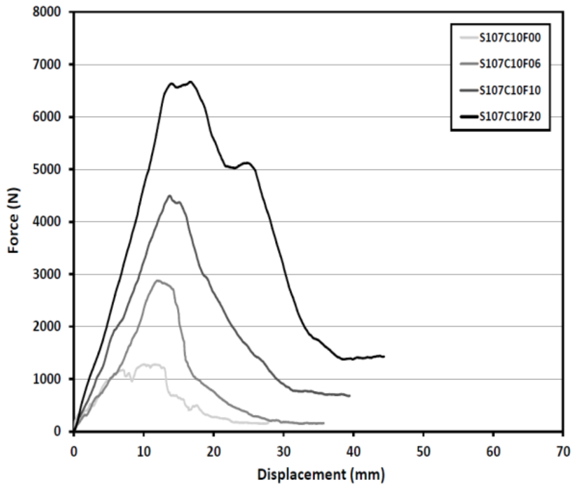


(a)

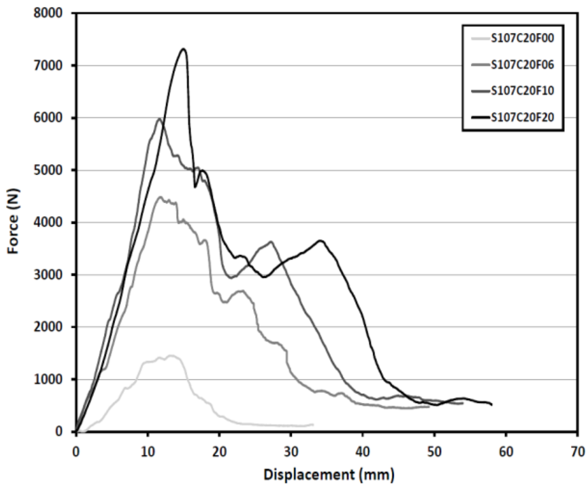


(b)

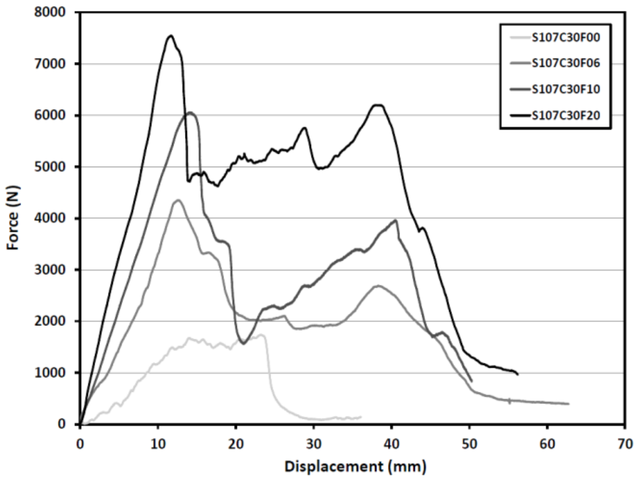


(c)

Fig. 5. Piercing force-displacement curves of specimens with 0.7 g/cm$^3$ foam core density for a) 10 mm, b) 20 mm and c) 30 mm foam core thickness

Piercing force-displacement curves of sandwich structures are not very smooth and exhibit some serrations, especially between two peaks. The main reason for these serrations is the presence of SiC particles in Al alloy matrix and formation of a brittle Al/SiCp composite structure. According to the mechanical properties of matrix materials, metallic foams include three types, i.e. elastic, plastic and brittle. The brittleness of Al/SiCp composites is generally more than that of Al alloy, therefore, Al/SiCp composite foams behave like the brittle foams. When the indenter force on Al/SiCp composite foams reaches the maximum, it comes into the collapse plateau region. With the indenter perforation, parts of cell walls suddenly produce cracks and brittle rupture, the space inside these cells decrease, and the force level also reduce suddenly. The force frequently rises and decreases and serrations occur.

***b) Peak piercing force and absorbed energy***

The total energy absorbed by each sandwich panel is the area under the force-displacement curve. For each sample peak piercing force, total absorbed energy and specific absorbed energy in terms of mass are listed in Table 1. It is obvious that S106C10F20 and S107C10F20 specimens have the highest specific absorbed energy in terms of mass.

**1. Effect of face-sheet thickness:** The effect of face-sheet thickness on peak piercing force and absorbed energy of sandwich panels in different foam core densities and thicknesses are shown in Fig. 6 and Fig. 7. It is obvious that in the same foam core density and thickness, thicker face-sheets with higher resistance against perforation force resulted in higher peak piercing force and total absorbed energy. For the range of foam cores and face-sheets thicknesses tested, the peak piercing force is almost linearly proportional to the face-sheet thickness. Increasing the face thickness, the peak piercing force of the sandwich panels with thicker foam cores tend to converge. This suggests that for panels with thicker face-sheets, the relative contribution from the core thickness on piercing force-displacement behavior of sandwich panels decreases.

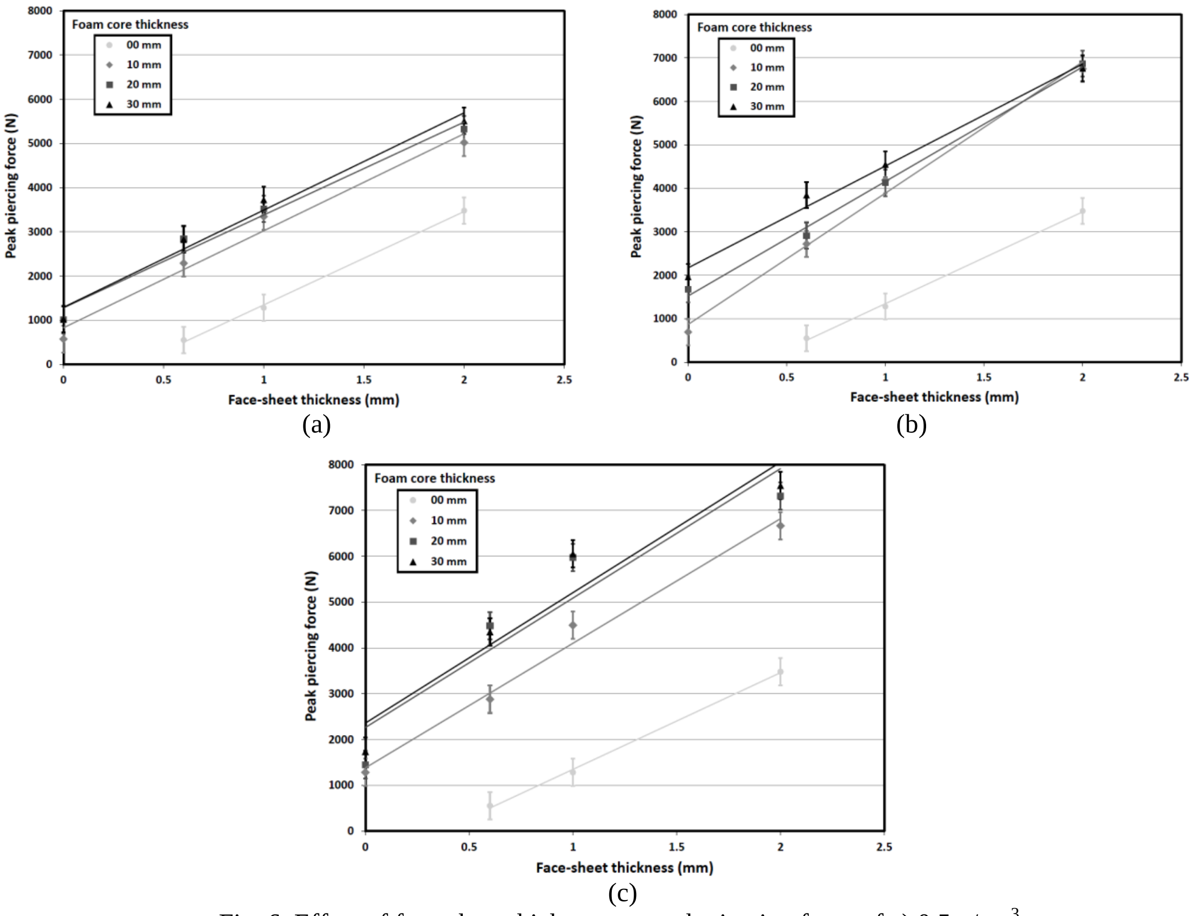


Fig. 6. Effect of face-sheet thickness on peak piercing force of a) 0.5 g/cm$^3$, b) 0.6 g/cm$^3$ and c) 0.7 g/cm$^3$ foam core density specimens

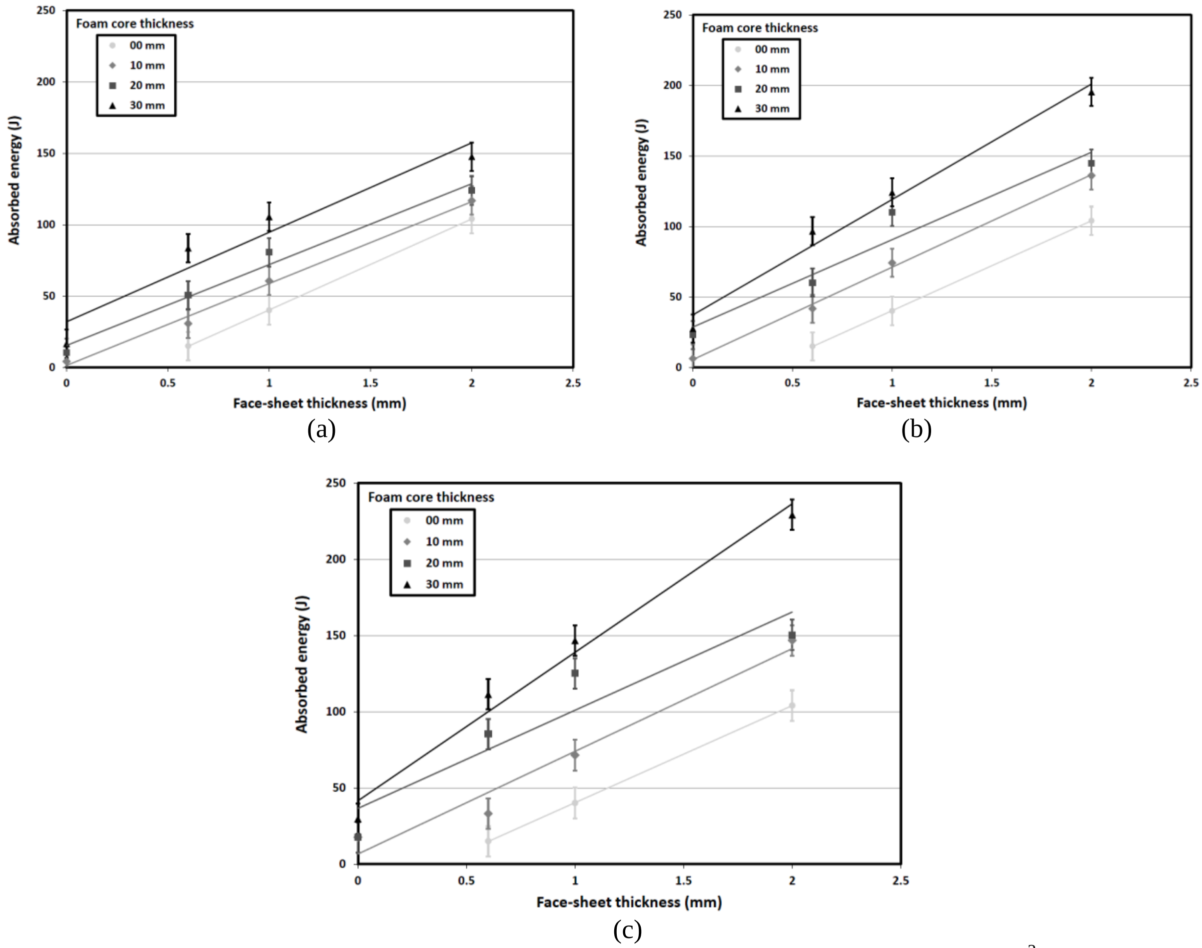


Fig. 7. Effect of face-sheet thickness on total absorbed energy of a) 0.5 g/cm$^3$, b) 0.6 g/cm$^3$ and c) 0.7 g/cm$^3$ foam core density specimens

**2. Effect of foam core thickness:** The foam core is crushed and densified between two peaks on the force-displacement curves. Thus increasing core thickness in the same density and face-sheet thickness expands the distance between two peaks and results in higher total energy absorption. Moreover, for sandwich panels with thin face-sheets, thick foam core results in a relatively higher peak piercing force level; while for sandwich panels with thicker face-sheets, core thickness does not show a considerable effect on force level. As mentioned above the relative contribution from the core thickness on piercing force-displacement behavior of sandwich panels decreases with increasing face-sheet thickness. Figures 8 and 9 respectively exhibit the effect of foam core thickness on peak piercing force and total energy absorption of sandwich panels in different foam core densities and face-sheet thicknesses.

**3. Effect of foam core density:** Plots of peak piercing force and energy absorption against foam core density in different face-sheet and foam core thicknesses are shown in Fig. 10 and Fig. 11. Figures reveal an approximately linear increasing relationship between density and both peak piercing force and total absorbed energy because of the increasing volume of bulk material and so, higher level of resistance against perforation force. This is in agreement with Fig. 4b and the effect of foam density on plateau stress.

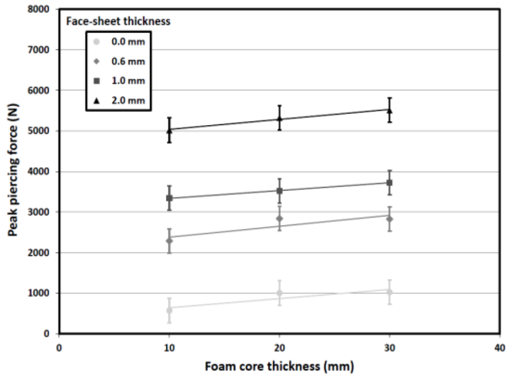


(a)

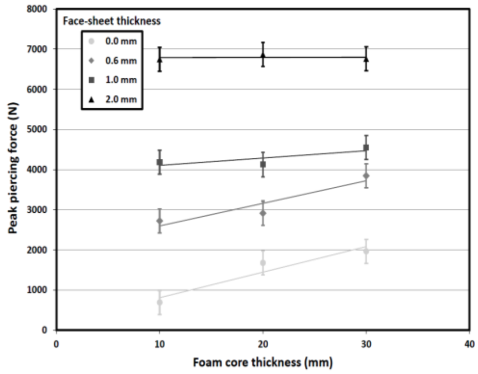


(b)

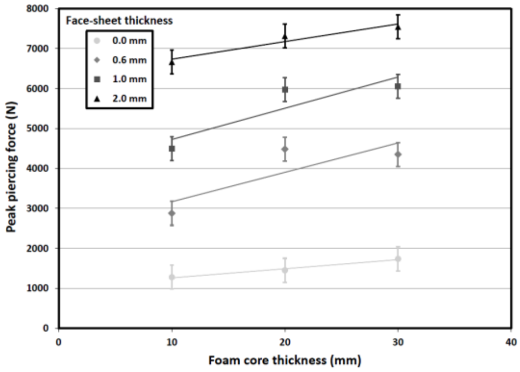


(c)

Fig. 8. Effect of foam core thickness on peak piercing force of a) 0.5 g/cm$^3$, b) 0.6 g/cm$^3$ and c) 0.7 g/cm$^3$ foam core density specimens

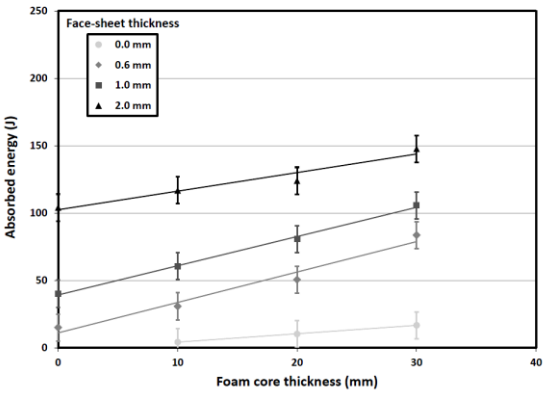


(a)

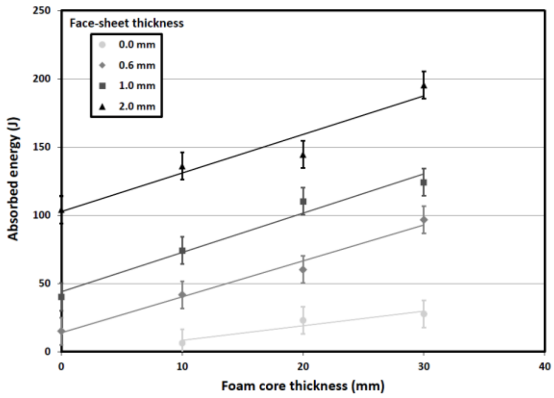


(b)

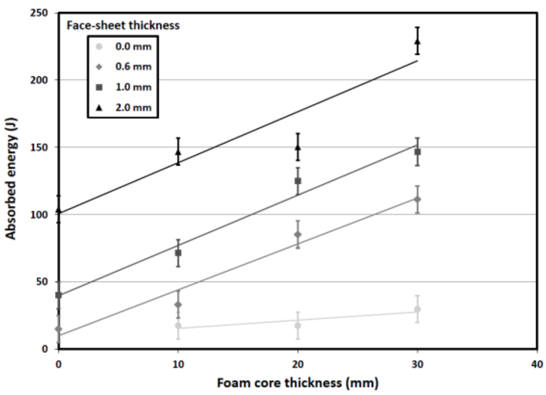


(c)

Fig. 9. Effect of foam core thickness on total absorbed energy of a) 0.5 g/cm$^3$, b) 0.6 g/cm$^3$ and c) 0.7 g/cm$^3$ foam core density specimens

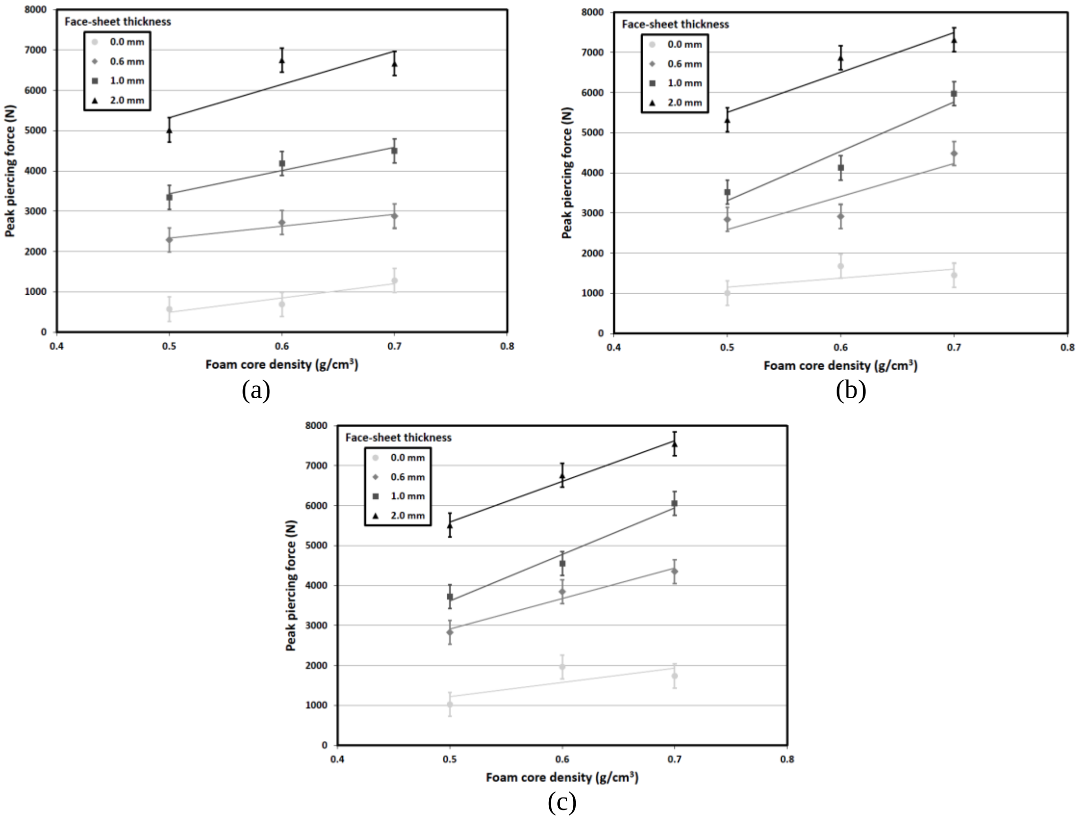


Fig. 10. Effect of foam core density on peak piercing force of specimens with a) 10 mm, b) 20 mm and c) 30 mm foam core thickness

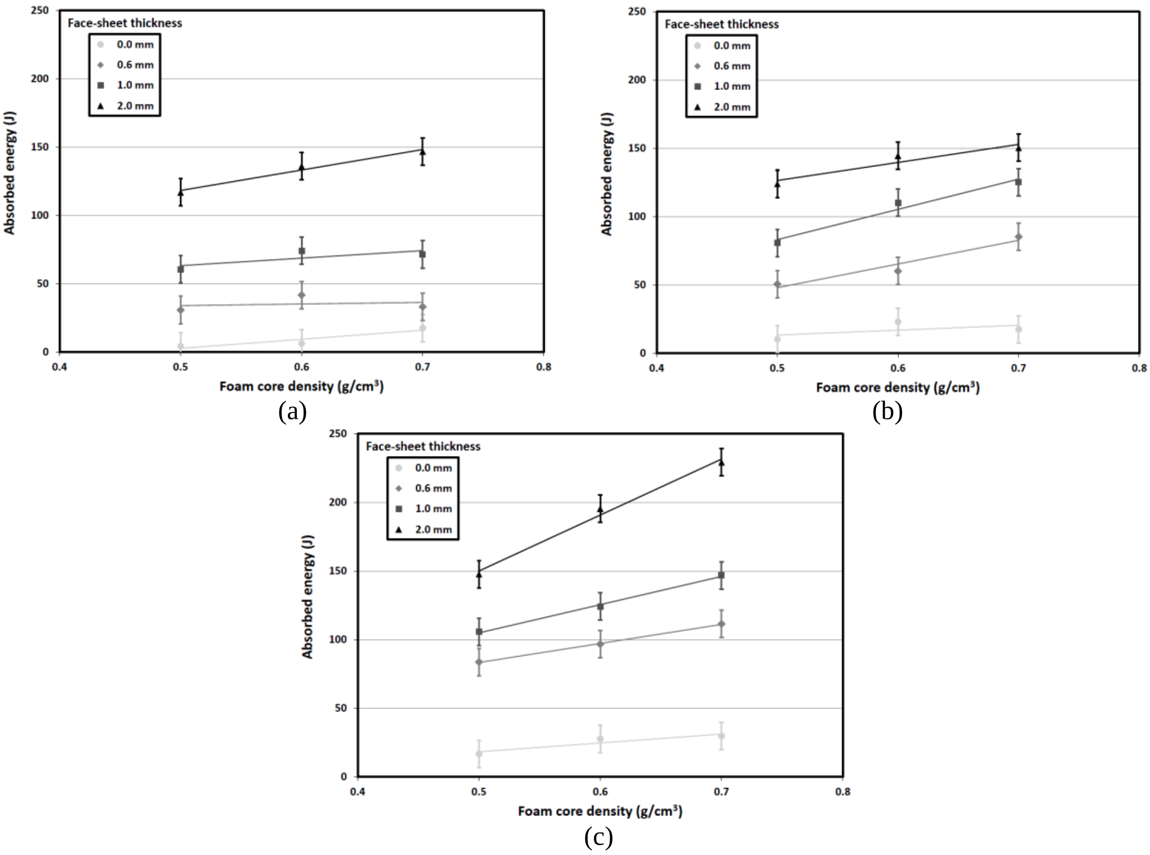


Fig. 11. Effect of foam core density on total absorbed energy of specimens with a) 10 mm, b) 20 mm and c) 30 mm foam core thickness

## 4. CONCLUSION

In this paper, quasi-static perforation tests were carried out on different sandwich panels with aluminum composite foam core and aluminum face-sheets. Results of the experiments are listed below:

1) Perforation process is divided into three stages: front face failure, core failure, and back face failure.

2) Thicker face-sheets in the same foam core density and thickness resulted in higher peak piercing force and total absorbed energy.

3) Increasing core thickness in the same density and face-sheet thickness expands the distance between two peaks and results in higher total energy absorption.

4) For sandwich panels with thin face-sheets, thick foam core results in a relatively higher peak piercing force level.

5) Core thickness does not show a considerable effect on force level for sandwich panels with thick face-sheets.

6) An increasing linear relationship is exhibited between density and both peak piercing force and total absorbed energy.

## REFERENCES

1. Ashby, M. F., Evans, A. G., Fleck, N. A., Gibson, L. J., Hutchinson, J. W. & Wadley, H. N. G. (2000). *Metal foams: a design guide*. Cambridge University Press, NewYork.
2. Degischer, H. P. & Kriszt, B. (2002). *Handbook of cellular metals*. Weinheim, Wiley-VCH.
3. Banhart, J. (2001). Manufacture, characterization and application of cellular metals and metallic foams. *Progress in Material Science*, Vol. 46, pp. 559-632.
4. Gibson, L. J. & Ashby, M. F. (1997). *Cellular solids: structure and properties*. 2nd ed., Cambridge University Press.
5. Lu, G. & Yu, T. X. (2003). *Energy absorption of structures and materials*. Cambridge: Woodhead Publishing Limited.
6. Cantwell, W. J. & Kiratisaevee, H. (2005). *Low-velocity impact response of high performance aluminum foam sandwich structures, Journal of Reinforced Plastics and Composites*, Vol. 24, pp. 1057-1072.
7. Mohan, K., Seow, H. P., Sridhar, I. & Yip, T. H. (2007). *Effects of face sheet material in the indentation response of metallic foams*. *Journal of Materials Science and Engineering*, Vol. 42, pp. 3714-3723.
8. Lu, G., Shen, J., Hou, W., Ruan, D. & Ong, L. S. (2008). Dynamic indentation and penetration of aluminum foams. *International Journal of Mechanical Sciences*,Vol. 50, pp. 932-943.
9. Ruan, D., Lu, G. & Wong, Y. C. (2010). *Quasi-static indentation tests on aluminum foam sandwich panels*. *Composite Structures*, Vol. 92, pp. 2039-2046.
10. Hou, W., Zhu, F., Lu, G. & Fang, D. (2010). *Ballistic impact experiments of metallic sandwich panels with aluminum foam core. International Journal of Impact Engineering*, Vol. 37, pp. 1045-1055.
11. Xie, Z., Zheng, Z. & Yu, J. (2013). Localized indentation of sandwich panels with metallic foam core: Analytical models for two types of indenters. *Composites: Part B*, Vol. 44, pp. 212-217.
12. Rajaneesh, A., Sridhar, I. & Rajendran, S. (2014). Relative performance of metal and polymeric foam sandwich plates under low velocity impact. *International Journal of Impact Engineering*, Vol. 65, pp. 126-136.
13. Altenaiji, M., Guan, Z.W., Cantwell, W.J., Zhao, Y. & Schleyer, G.K. (2014). Characterisation of aluminium matrix syntactic foams under drop weight impact. *Materials & Design*, Vol. 59, pp. 296-302.

14. Golestanipour, M., Amini Mashhadi, H., Abravi, M. S., Malekjafarian, M. & Sadeghian, M. H. (2011). Manufacturing of Al/SiCp composite foams using calcium carbonate as foaming agent. *Materials Science and Technology*, Vol. 27, pp. 923-927.
15. Solhjoo, S., Simchi, A. & Aashuri, H. (2012). Molecular dynamics simulation of melting, solidification and remelting processes of aluminum. *Iranian Journal of Science and Technology-Transactions of Mechanical Engineering*, Vol. 36, pp. 13-23.